

Calorimetric and ^{23}Na MAS NMR study of the phase diagram of $\text{NaNb}_{1-x}\text{Ta}_x\text{O}_3$ solid solutions

*I.P.Aleksandrova, Yu.N.Ivanov, V.S.Bondarev**,
A.A.Sukhovskii, V.N.Voronov

L.Kirensky Institute of Physics, Russian Academy of Sciences,
Siberian Branch, 660036 Krasnoyarsk, Russia

*Siberian Federal University, 660041 Krasnoyarsk, Russia

Received November 10, 2009

The heat capacity of $\text{NaNb}_{1-x}\text{Ta}_x\text{O}_3$ solid solutions was measured in the temperature range 100 to 770 K. The step-like change of phase transition temperature is observed in the T - x phase diagram at concentration $x = 0.55$. The obtained results are in a good agreement with the data of dielectric studies. The ^{23}Na MAS NMR spectra were obtained at Larmor frequency 79.35 MHz using a Bruker AVANCE 300 spectrometer. The quadrupolar coupling constant, ($C_Q = e^2qQ/h$) and asymmetry parameter (η) were determined by computer fitting of the NMR line shape using the DMFit software. The found parameters show that solid solution structure is NaTaO_3 -based at $0.7 < x \leq 1$ and NaNbO_3 -based at $0 \leq x \leq 0.5$. The spectra in the intermediate region ($0.5 < x \leq 0.7$) can be described at a reasonable accuracy when assuming the coexistence of NaTaO_3 and NaNbO_3 structures.

Исследована теплоемкость твердых растворов $\text{NaNb}_{1-x}\text{Ta}_x\text{O}_3$ в интервале температур 100–770 К. На фазовой диаграмме x - T отмечено ступенчатое изменение температуры фазового перехода при $x = 0,55$. Полученные результаты хорошо согласуются с данными диэлектрических исследований. Спектры ЯМР MAS ^{23}Na получены с использованием спектрометра Bruker AVANCE 300 на ларморовской частоте 79,35 МГц. Константа квадрупольной связи ($C_Q = e^2qQ/h$) и параметр асимметрии (η) определялись путем компьютерной аппроксимации формы кривой ЯМР с использованием программного обеспечения DMFit. Найденные параметры свидетельствуют, что твердый раствор имеет структуру на основе NaTaO_3 при $0,7 < x \leq 1$ и на основе NaNbO_3 при $0 \leq x \leq 0,5$. Спектры в промежуточной области ($0,5 < x \leq 0,7$) можно описать с удовлетворительной точностью, исходя из предположения о сосуществовании структур NaTaO_3 и NaNbO_3 .

1. Introduction

Some binary solid solutions NaNbO_3 - ABO_3 are known to exhibit the relaxor properties when the second component concentration exceeds a certain value x_0 . The $\text{NaNb}_{1-x}\text{Ta}_x\text{O}_3$ solid solutions belong to this group. According to the literature data [1], sodium niobate undergoes six phase transitions with the following phase sequence: high-temperature (PE) cubic $\text{Pm}\bar{3}\text{m} \rightarrow$ (PE) tetragonal $\text{P4}/\text{mbm} \rightarrow$ (PE) orthorhombic $\text{Ccm} \rightarrow$ (PE) orthorhombic $\text{Pnm} \rightarrow$ (AFE)

orthorhombic $\text{Pnm} \rightarrow$ (AFE) orthorhombic $\text{Pbcm} \rightarrow$ (FE) rhombohedral $\text{R}\bar{3}\text{c}$. As to sodium tantalate, three phase transitions are known to occur at 890, 835, and 700 K [2]. Before, the concentration phase diagram (T - x) of the $\text{NaNb}_{1-x}\text{Ta}_x\text{O}_3$ solutions was studied mainly by dielectric methods [3, 4, 5]. In NaNbO_3 , the anomalies of permittivity ϵ' are observed at the phase transition between the antiferroelectric Pnm and Pbcm structures at 633 K and at the ferroelectric phase transition between the an-

tiferroelectric Pbcm phase and the polar R3c phase at 73 K [1, 3].

In the $\text{NaNb}_{1-x}\text{Ta}_x\text{O}_3$ solid solutions, the first-order Pmnm – Pbcm transition line is observed at increasing Ta concentration up to the end point at $x = x_0 \approx 0.6$ [3]. However, there is an opinion that the transition temperature drops by more than 200 K at x_0 and continues to $x \approx 0.8$ [4]. The ε' maximum pronounced enough in the range $x < x_0$ becomes diffuse at $x > x_0$. An evident frequency dispersion of permittivity and the transition temperature shift toward higher temperatures are observed as the measuring frequency increases. These features of the permittivity anomaly in the $\text{NaNb}_{1-x}\text{Ta}_x\text{O}_3$ solutions are much weaker than those in classical Pb-containing relaxors. It should be noted, however, that even a small additive of a third component, Li for example, increases the permittivity and the transition temperature considerably, which makes these compounds attractive for applications. As far as we know, the phase diagram T - x of $\text{NaNb}_{1-x}\text{Ta}_x\text{O}_3$ in the range $x > x_0$ was not studied by methods providing information at the structure level. In our case, such methods of the local structure study as the traditional nuclear magnetic resonance (NMR) and electron spin resonance (ESR) cannot be used because those require sufficiently large single crystals. In this study, we use the "magic angle spinning" (MAS) NMR method which can provide information on the structure when using polycrystal samples. The important point is that the MAS method provides a high resolution in the NMR spectra. In order to investigate the T - x phase diagram line in a wide temperature range, calorimetric measurements were performed.

2. Experimental

The samples of $\text{NaNb}_{1-x}\text{Ta}_x\text{O}_3$ ($x = 0, 0.2, 0.3, 0.55, 0.6, 0.7, 0.8, 0.9$ and 1.0) solid solutions were prepared by the high-temperature solid-state synthesis. The samples were pressed at 15 MPa, preliminary calcinated at 1220 K, and synthesized at 1420 K. The heat capacity of $\text{NaNb}_{1-x}\text{Ta}_x\text{O}_3$ ($x = 0, 0.2, 0.3, 0.55, \text{ and } 0.6$) solid solutions was measured in the 100 to 770 K temperature range using a differential scanning calorimeter (DSC) in the course of both heating and cooling at the rate of 16 K/min. The ceramic samples (0.1–0.2 g) were packed in an aluminum container. The error inherent in this method (~15 %) is sub-

stantially larger than that in other calorimeters, for example, in an adiabatic calorimeter. The scatter of experimental points from a smoothed curve did not exceed 1 %. In the 4–290 K range, the heat capacities of $\text{NaNb}_{0.2}\text{Ta}_{0.8}\text{O}_3$ and $\text{NaNb}_{0.1}\text{Ta}_{0.9}\text{O}_3$ were measured with a Physical Property Measurement System (PPMS, Quantum Design). The sample mass was 0.029 and 0.041 g, respectively. To provide a good thermal contact between the platform and a sample, vacuum low-temperature lubricant (Apiezon) in 0.35 mg amount was used. The measurement accuracy depends on the heating method and amounts to (0.1–0.3) %.

The ^{23}Na MAS NMR spectra were measured using an AVANCE 300 pulse spectrometer at a Larmor frequency of 79.4 MGz. The samples were placed into a 4-mm zirconia container and rotated at a "magic" angle of 54.7° to the external magnetic field at the 15 kHz frequency. If the rotation speed exceeds, as in our case, the value of the dipole-dipole interaction, then the latter is averaged to zero and a high-resolved spectrum is observed in a solid. In the high-resolved spectrum, an isotropic part of the chemical shift and the second-order quadrupole shift of the central ($-1/2 \leftrightarrow 1/2$ transition) component of the ^{23}Na NMR spectrum are retained. The specific shape of the high-resolution line in the polycrystal samples with the quadrupole interaction permits to determine the parameters of the quadrupole interaction tensors at a good accuracy even in the presence of overlapping lines from several structurally nonequivalent sodium sites in a structure.

3. Results of the measurements

Fig. 1 shows the study results of a $\text{NaNb}_{1-x}\text{Ta}_x\text{O}_3$ solid solution with $x = 0.9$. The curve describing the temperature dependence of heat capacity does not exhibit clearly manifested anomalies typical of traditional phase transitions. However, in the temperature region 50–200 K, a broad blurred anomaly in $C_p(T)$ at $T = 90 \pm 2$ K is observed. To analyse these features in more detail, the anomalous ΔC_p and lattice C_L contributions to the total heat capacity should be separated. This procedure was carried out using a simple model describing the lattice heat capacity of a compound by a combination of the Debye and Einstein functions (dashed line in Fig. 1).

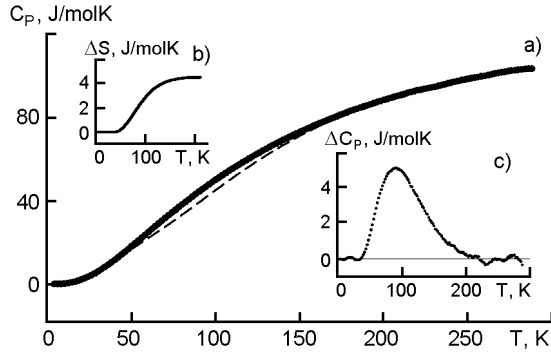


Fig. 1. a) temperature dependence of $\text{NaNb}_{0.1}\text{Ta}_{0.9}\text{O}_3$ heat capacity. Dashed line, the lattice heat capacity; b) temperature dependence of excess specific heat; c) temperature dependence of transition entropy.

$$C_L(T) = A \left(\frac{T}{\Theta_D} \right)^3 \int_0^{\Theta_D/T} x^4 \frac{\exp(x)}{(\exp(x) - 1)^2} dx + B \left(\frac{\Theta_E}{T} \right)^2 \frac{\exp\left(\frac{\Theta_E}{T}\right)}{\left(\exp\left(\frac{\Theta_E}{T}\right) - 1\right)^2}, \quad (1)$$

where A and B are the fitting parameters and Θ_D and Θ_E are the characteristic Debye and Einstein temperatures. It is to note that when extrapolating to the high-temperature area, the heat capacity [described by Eq.(1)] tends to the classical value following from the Dulong-Petit law:

$$C_V = 3N_A \cdot k_B, \quad (2)$$

where N_A is the Avogadro number and k_B is the Boltzmann constant.

In the temperature area under consideration, the heat capacity is already poorly sensitive to fine details of the vibration spectrum and the approximation of the lattice contribution carried out in that way is quite justified. Thus, anharmonic contributions and distinction $C_p(T)$ and $C_v(T)$ were not considered, as this difference is as a rule insignificant due to low thermal expansion coefficients of the NaNbO_3 -based solid solutions. The anomalous component of heat capacity $\Delta C_p = C_p - C_L$ shown in Fig. 1b reaches only $\sim 5.0 \text{ J}\cdot\text{mol}^{-1}\cdot\text{K}^{-1}$ or $\sim 10\%$ of lattice heat capacity $C_L(T)$. The entropy change associated with the anomalous behaviour of heat capacity, determined as $\Delta S = \int (\Delta C_p/T) dT$, is shown in Fig. 1c. The

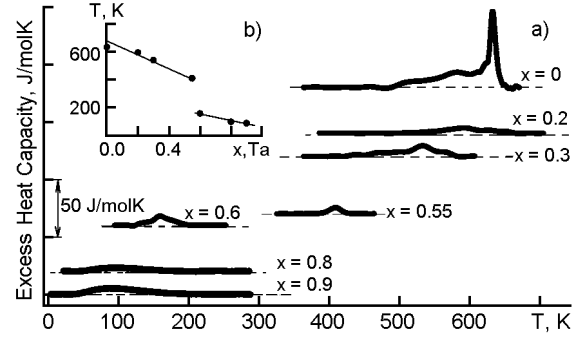


Fig. 2. a) temperature dependence of excess heat capacity for different Ta concentrations; b) change of phase transition temperatures with Ta concentration.

small value of $\Delta S \approx 4.5 \text{ J}\cdot\text{mol}^{-1}\cdot\text{K}^{-1} \approx R \ln(2)$ demonstrates clearly the displacive nature of crystal phase changes.

Fig. 2 displays the temperature dependence of the excess heat capacity calculated after extraction of the lattice heat capacity for all the $\text{NaNb}_{1-x}\text{Ta}_x\text{O}_3$ solid solutions. The temperature dependence of the lattice heat capacity in the differential calorimetric study was approximated by a smooth polynomial function. This function coincided with the experimental curve outside the heat capacity abnormal behavior. As would be expected according to the dielectric data, the first-order phase transition ($\text{Pbcm} \rightarrow \text{Pmmn}$) is observed at $T = 633 \text{ K}$ in the solid solution with $x = 0$. In this case, the total entropy change is $\Delta S \approx (3.2 \pm 0.4) \text{ J}\cdot\text{mol}^{-1}\cdot\text{K}^{-1}$. Such a small entropy change indicates a substantial role being played by displacive processes in the phase-transition mechanism. As the Ta concentration increases, the heat capacity anomaly decreases, diffuses, and displaced towards low temperatures. The concentration $x = 0.55$ corresponds to the last experimentally registered point of the first-order transition ($\text{Pbcm} \rightarrow \text{Pmmn}$). At a further increase of Ta concentration ($x = 0.6-0.9$), the only low-temperature heat capacity anomaly is observed. This anomaly is displaced in low temperature area with increasing x . The anomaly strongly broadens with the increasing Ta concentration and above $x = 0.9$ it is nearly impossible to extract the excess heat capacity from the lattice one. The $T-x$ phase diagram of $\text{NaNb}_{1-x}\text{Ta}_x\text{O}_3$ obtained from the calorimetric data is presented in Fig. 2b. The obtained results of phase transition temperature are in a

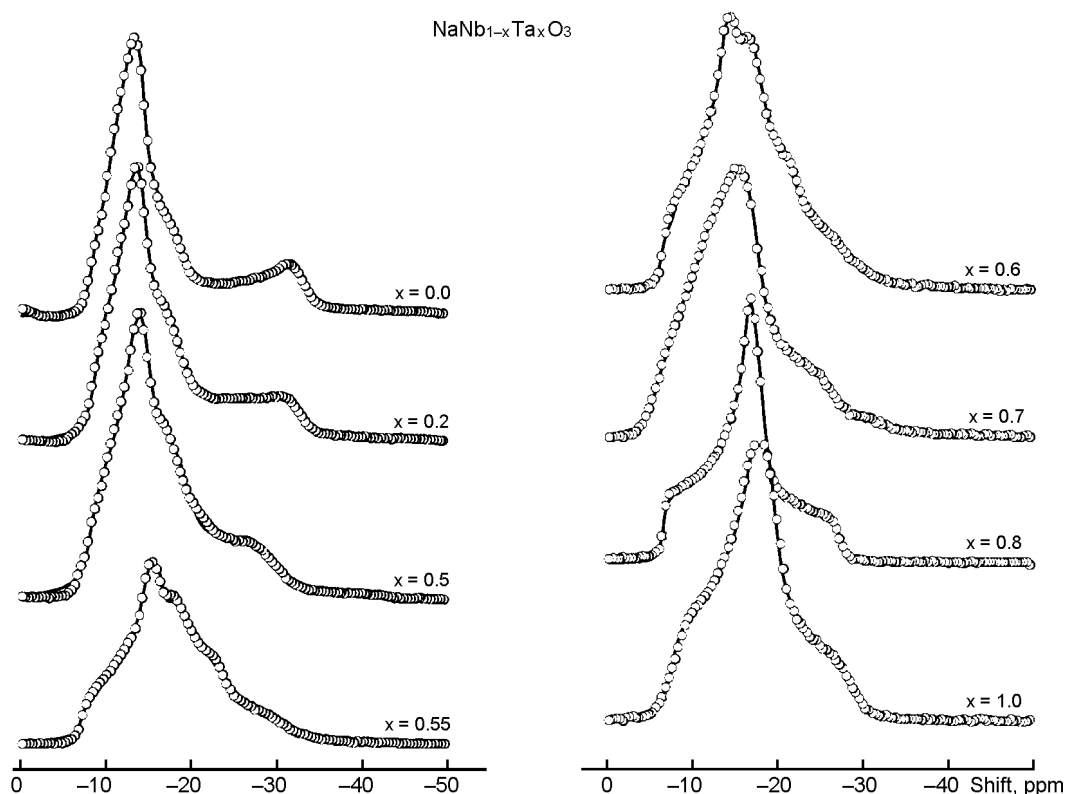


Fig. 3. The ^{23}Na NMR MAS spectra in $\text{NaNb}_{1-x}\text{Ta}_x\text{O}_3$ solid solutions.

good agreement with the data of dielectric studies [4].

Fig. 3 shows the ^{23}Na MAS spectra taken at room temperature for several solid solutions of a general formula $\text{NaNb}_{1-x}\text{Ta}_x\text{O}_3$ at Ta concentration x from 0 to 1. At room temperature, the NaNbO_3 structure is in the antiferroelectric Pbcm phase with two lattice positions of ^{23}Na in the unit cell quadruplicated along the c direction [1, 5]. Thus, the NaNbO_3 MAS spectrum should be a superposition of the lines from the two lattice sites: Na1 in the special (4c) position and Na2 in the general (4d) position (Fig. 4).

The spectra of the solid solutions in the concentration range from 0 to 0.5 vary gradually with increasing x , keeping the shape typical of NaNbO_3 . However, at $x = 0.55$, the spectrum line shape changes drastically. High resolution of the spectrum obtained with MAS makes it possible to resolve the spectrum of the Pbcm phase and a new line occurring from a certain third Na3 site at $x = 0.55$. The majority of the spectral intensity is concentrated in the line belonging to the Na3 position. The spectrum consisting of three overlapping lines is observed in the range from $x = 0.55$ to $x = 0.7$. At $x = 0.8$ and 0.9, there is the only

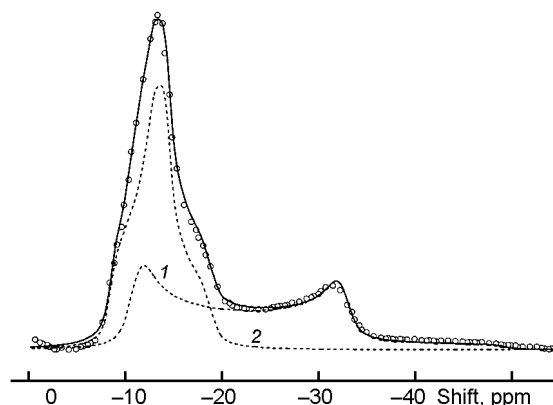


Fig. 4. The decomposition of experimental ^{23}Na NMR MAS spectrum of NaNbO_3 . Two components correspond to Na1 (1) and Na2 (2) positions.

line from the Na3 nucleus located in the general position in the cell.

The high-resolved spectra were processed using the DMFit software [6]. The quadrupole coupling constants C_{Qi} , asymmetry parameters of the electric field gradient (EFG) tensor η_i , and integral intensities A_i of the spectrum components, are varied during fitting of the model spectrum to the experimental NMR spectrum. The results of the analysis are given in the Table. Parameters

Table. Analysis results of the experimental NMR spectrum.

x	A_1	$C_Q(\text{kHz})$	η_1	A_2	$C_Q(\text{kHz})$	η_2	A_3	$C_Q(\text{kHz})$	η_3
0.0	0.5	2115	0.0	0.5	990	0.9	–	–	–
0.2	0.4	1756	0.0	0.6	980	0.8	–	–	–
0.5	0.4	1544	0,0	0.6	1040	0.8	–	–	–
0.55	0.1	1679	0.2	0.2	1200	0.9	0.7	1223	0.9
0.6	0.1	1520	0.4	0.1	1200	0.9	0.8	1269	0.9
0.7	0.1	1619	0.4	0.1	1120	0.9	0.8	1386	0.9
0.8	–	–	–	–	–	–	1	1359	0.9
1.0	–	–	–	–	–	–	1	1396	0.9

A , C_Q (kHz), and η were determined at the accuracy of ± 0.1 , ± 100 , and ± 0.1 , respectively.

According to the Table, the solid solutions in the concentration range from 0 to 0.5 retain the symmetry of the Na1 and Na2 sites existing in Pbcm space group of NaNbO_3 structure. Note that the Na1 spectrum shape corresponds to the theoretical line with two maxima typical of the parameter $\eta = 0$, while the Na2 spectrum is characteristic of the general position of a nucleus with $\eta \approx 0.8$ (Fig. 4). As is known, the asymmetry parameter is zero when the observed nucleus is located on the symmetry axis of third or higher order. In our case, zero value η in the Pbcm phase is caused by the subcell cubic pseudosymmetry. When Ta enters the NaNbO_3 lattice, the quadrupole coupling constant of the Na1 nucleus reduces and that of the Na2 nucleus somewhat increases with x . At $x > 0.5$, the nonzero asymmetry parameter of the EFG tensor occurs on the Na1 nuclei and reaches the value $\eta = 0.4$ at $x = 0.7$. Such a variation in the EFG tensor parameters originates from strong local distortions of the Pbcm phase structure in the solid solutions under study.

The sharp change in the spectrum shape (Fig. 2) at $x = 0.55$, as is seen from the Table, results from jump-like integral intensity drop of the spectrum from the Na1 and Na2 nuclei down to 0.1 ± 0.1 . The main integral spectrum intensity at $x \geq 0.55$ is focused in the Na3 line, which grows within $x = 0.55\text{--}0.7$ attaining 1 at $x = 0.8$. At the concentrations $x = 0.8, 0.9$, and 1, parameters A_3 , C_{Q3} , and η_3 have constant values. The quadrupole coupling constant and the EFG tensor asymmetry parameter on Na3 nucleus in this concentration range correspond with high accuracy to the known values for NaTaO_3 [7].

4. Conclusion

The above results demonstrate the existence of two areas with different structures in the T - x phase diagram of the $\text{NaNb}_{1-x}\text{Ta}_x\text{O}_3$ solid solutions, depending on Ta concentration. In the concentration range $x = 0\text{--}0.55$, the solid solution structure below 633 K retains the Pbcm space group inherent in the NaNbO_3 structure. Accordingly, in those concentration and temperature ranges the line of the first-order transitions between the antiferroelectric Pbcm and Pnmm phases is observed. This line has the end point at $x = 0.55 \pm 0.05$. Note that transition line of the ferroelectric transition $\text{R3c} \leftrightarrow \text{Pbcm}$ observed in NaNbO_3 at 245 K upon heating was not revealed during our calorimetric measurements at $x < 0.55$. This is possibly related to strong blurring of the thermal anomaly due to the coexistence of the R3c and Pbcm phases in a wide temperature range [1]. At $x > 0.55$ and below 700 K, the solid solutions are formed on the basis of the NaTaO_3 structure with the Pbnm space group. In the low-temperature region, the second-order transition line is observed that limits the region where the Pbnm phase exists (Fig. 2b). This transition occurs to the ferroelectric structure whose space group is being refined by us. With increasing x , a strong broadening of the thermal anomaly is observed in this region. The phase transition may be observed up to $x = 0.9$. According to the literature data, at $x = 1$, there are no phase transitions below room temperature. Within the range $x = 0.55\text{--}0.7$, the ^{23}Na spectra show the coexistence of the NaNbO_3 - and NaTaO_3 -based solid solutions. Perhaps the dielectric properties typical of the relaxor ferroelectrics in the $\text{NaNb}_{1-x}\text{Ta}_x\text{O}_3$ series have the same origin as the ferroelectric transition in NaNbO_3 [1], i.e., occur due to the coexis-

tence of phases with free energy difference on a level of thermal fluctuations.

Acknowledgements. This work was supported by a grant from the President of the Russian Federation for support of leading scientific schools (NSh-4645.2010.2) and Siberian Branch of RAS program (project 2.5.1).

References

1. S.N.Mishra, N.Choudhury, S.L.Chaplot et al., *cond-mat/0703365*.
2. B.J.Kennedy, A.K.Prodjosantoso, C.J.Howard, *J. Phys.:Condens.Matter.*, **11**, 6319 (1999).
3. N.N.Krainik, *Izv.AN SSSR, Ser.Fiz.*, **22**, 1492 (1958).
4. I.P.Raevski, S.A.Prosandeev, *cond-mat/0208314*.
5. H.Ywasaki, *Rev.Elekt.r.Commun.Lab.*, **12**, 469 (1964).
6. D.Massiot, F.Fayon, M.Capron et al., *Magn. Reson. Chem.*, **40**, 70 (2002).
7. S.E.Ashbrook, L.Le Polles, R.Gautier et al., *Phys.Chem.Chem.Phys.*, **8**, 3423 (2006).

Дослідження фазової діаграми твердих розчинів $\text{NaNb}_{1-x}\text{Ta}_x\text{O}_3$ методами калориметрії та ЯМР MAS ^{23}Na

*І.П.Александрова, Ю.Н.Іванов, В.С.Бондарев,
А.А.Суховський, В.Н.Воронов*

Досліджено теплоємність твердих розчинів $\text{NaNb}_{1-x}\text{Ta}_x\text{O}_3$ в інтервалі температур 100–770 К. На фазовій діаграмі x – T відзначено ступінчасту зміну температури фазового переходу при $x = 0,55$. Одержані результати добре узгоджуються з даними діелектричних досліджень. Спектри ЯМР MAS ^{23}Na одержано з використанням спектрометра Bruker AVANCE 300 на ларморівській частоті 79,35 МГц. Константа квадрупольного зв'язку ($C_Q = e^2qQ/h$) та параметр асиметрії (η) визначалися шляхом комп'ютерної апроксимації форми кривої ЯМР з використанням програмного забезпечення DMFit. Знайдені параметри свідчать, що твердий розчин має структуру на основі NaTaO_3 при $0,7 < x \leq 1$ та на основі NaNbO_3 при $0 \leq x \leq 0,5$. Спектри у проміжній області ($0,5 < x \leq 0,7$) можна описати із задовільною точністю, виходячи з припущення про співіснування структур NaTaO_3 та NaNbO_3 .